Available online at www.sciencedirect.com
ScienceDirect
Journal of Computational Physics 227 (2007) 755–762
JOURNAL OF COMPUTATIONAL PHYSICS
www.elsevier.com/locate/jcp

Inverse scattering by a continuation method with initial guesses from a direct imaging algorithm ☆

Gang Bao [a,*], Songming Hou [b], Peijun Li [c]

[a] Department of Mathematics, Michigan State University, East Lansing, MI 48824, United States
[b] Department of Mathematics and Statistics, Louisiana Tech University, Ruston, LA 71272, United States
[c] Department of Mathematics, University of Michigan, Ann Arbor, MI 48109, United States

Received 3 April 2007; received in revised form 27 June 2007; accepted 15 August 2007
Available online 5 September 2007

Abstract

A novel continuation method is presented for solving the inverse medium scattering problem of the Helmholtz equation, which is to reconstruct the shape of the inhomogeneous medium from boundary measurements of the scattered field. The boundary data is assumed to be available at multiple frequencies. Initial guesses are chosen from a direct imaging algorithm, multiple signal classification (MUSIC), along with a level set representation at a certain wavenumber, where the Born approximation may not be valid. Each update via recursive linearization on the wavenumbers is obtained by solving one forward and one adjoint problem of the Helmholtz equation.

Keywords: Continuation method; MUSIC; Inverse scattering

1. Introduction

Consider the Helmholtz equation in two dimensions

$$\Delta u^{\mathrm{t}}(\mathbf{x}) + k^2(1 + q(\mathbf{x}))u^{\mathrm{t}}(\mathbf{x}) = 0, \quad \mathbf{x} \in \mathbb{R}^2, \tag{1.1}$$

where u^{t} is the total electric field, k is the wavenumber, and $q(\mathbf{x}) > -1$ is the scatterer with a compact support. Assume that the scatterer is illuminated by plane waves

$$u^{\mathrm{i}}(\mathbf{x}) = \mathrm{e}^{\mathrm{i}k\mathbf{x}\cdot\mathbf{d}},$$

where $\mathbf{d}$ is the propagation direction. Evidently, such incident waves satisfy the homogeneous equation

☆ This research was supported in part by the NSF Grants DMS-0604790 and CCF-0514078, the ONR Grant N000140210365, and the National Science Foundation of China Grant 10428105.
* Corresponding author. Fax: +1 517 432 1562.
E-mail addresses: bao@math.msu.edu (G. Bao), shou@latech.edu (S. Hou), lipeijun@umich.edu (P. Li).

0021-9991/$ - see front matter © 2007 Elsevier Inc. All rights reserved.
doi:10.1016/j.jcp.2007.08.020

$$\Delta u^{\mathrm{i}} + k^2 u^{\mathrm{i}} = 0. \tag{1.2}$$

The total field u^{t} consists of the incident field u^{i} and the scattered field u^{s}:

$$u^{\mathrm{t}} = u^{\mathrm{i}} + u^{\mathrm{s}}.$$

It follows immediately from Eqs. (1.1) and (1.2) that the scattered field satisfies

$$\Delta u^{\mathrm{s}} + k^2(1+q)u^{\mathrm{s}} = -k^2 q u^{\mathrm{i}}. \tag{1.3}$$

In addition, the scattered field is required to satisfy the following Sommerfeld radiation condition

$$\lim_{r\to\infty} \sqrt{r}\left(\frac{\partial u^{\mathrm{s}}}{\partial r} - \mathrm{i}ku^{\mathrm{s}}\right) = 0, \quad r = |\mathbf{x}|,$$

uniformly along all directions $\mathbf{x}/|\mathbf{x}|$.

Given the incident field u^{i}, the direct scattering problem is to determine the scattered field u^{s} for the known scatterer $q(\mathbf{x})$, which has been well studied [12]. The present paper focuses on the inverse scattering problem. For simplicity, suppose that the scatterer takes a constant value inside the inhomogeneities of the region. The inverse medium scattering problem is to determine the inhomogeneities from the measurements of the scattered field u^{s}, for the given incident field u^{i}. More specifically, for a given constant q_0, the inverse problem is to reconstruct a compact domain Ω such that

$$q(\mathbf{x}) = \begin{cases} q_0 & \text{for } \mathbf{x} \in \Omega, \\ 0 & \text{for } \mathbf{x} \in \mathbb{R}^2 \setminus \Omega. \end{cases}$$

Let D, containing the compact support of the scatterer $q(\mathbf{x})$, be a bounded domain in $\mathbb{R}^2$ with boundary ∂D. The scattered field is measured at $\mathbf{x}_j \in \partial D$, $j = 1, \ldots, m$.

The inverse medium scattering problems arise naturally in diverse applications such as radar, sonar, geophysical exploration, medical imaging, and nondestructive testing [12]. There are two major difficulties associated with these inverse problems: the ill-posedness and the presence of many local minima. To overcome the difficulties, stable and efficient regularized recursive linearization methods are developed in [5,7,10,11] for solving the two-dimensional Helmholtz equation and the three-dimensional Maxwell's equations [3,4] in the case of full aperture data. We refer the reader to [2,6] for limited aperture data cases. Roughly speaking, these methods start from the weak scattering, where the Born approximation may be used to produce initial guesses. Updates are obtained by a continuation approach on the wavenumbers or on the spatial frequencies. For related results on the inverse scattering problem, the reader is referred to [13,19,16,18,21–23] and reference therein. Although the methods yield stable and accurate computational results, they nonetheless rely on the weak scattering assumption for initial guesses. Unfortunately, as indicated in computational experiments, if the weak scattering assumption is violated, for example when the starting frequency is not sufficiently low, the Born approximation might lead to an initial guess with which the continuation approach would converge slowly or even diverge. To resolve this difficulty, we propose in this work a continuation approach starting from an initial guess via the MUSIC algorithm and a level set representation at a fixed wavenumber, where the Born approximation may not be valid. The method requires multiple frequency scattering data, and the recursive linearization is a continuation procedure on the wavenumbers.

The paper is organized as follows. An initial guess is derived from the MUSIC algorithm and a level set representation in Section 2. In Section 3, a regularized recursive linearization method is proposed. Numerical examples are presented in Section 4. The paper is concluded with some general remarks in Section 5.

2. Initial guess

In this section, we discuss how to generate an initial guess for the proposed recursive linearization method. The MUSIC algorithm for extended scatterers proposed in [20] is used to generate an image for the shape of the scatterer. The MUSIC algorithm for point scatterers may be found in [15]. See also [1] for an up-to-date discussion on various types of mathematical imaging methods. The image may be further converted into a level set representation for the scatterer through image processing.

2.1. The MUSIC algorithm for extended scatterers

Consider plane incident waves illuminating from m evenly spaced angles with a certain wavenumber. The scattered fields are recorded on $\partial\Omega$ with the same m evenly spaced angles. The data collected forms an m-by-m matrix, denoted by P, which is known as the response matrix. For simplicity of discussion, here we have the incident plane wave directions coincide with the recorded scattered field directions. However, the MUSIC algorithm and our continuation method to be discussed later can both handle the general case where the number of incident plane wave directions is different from the number of recorded scattered field directions and the directions do not coincide.

Let $P = U\Sigma V^H$ be the singular value decomposition of the response matrix. Define the illumination vector

$$\mathbf{g}(\mathbf{x}) = [\mathrm{e}^{\mathrm{i}k\mathbf{x}\cdot\mathbf{d}_1}, \ldots, \mathrm{e}^{\mathrm{i}k\mathbf{x}\cdot\mathbf{d}_m}]^{\mathrm{T}},$$

where $\mathbf{d}_j$ are the propagation directions of incident waves and $\mathbf{x}$ is any point in the space. The MUSIC imaging function may be introduced:

$$I(\mathbf{x}) = \frac{1}{\|\mathbf{g}(\mathbf{x})\|_2^2 - \sum_{\ell=1}^{s}|\mathbf{g}(\mathbf{x})^H\mathbf{u}_\ell|^2}, \tag{2.1}$$

where $\mathbf{u}_\ell$ is the ℓth column of the matrix U and the number of singular vectors s that spans the signal space is determined by the resolution analysis based thresholding algorithm in [20].

The imaging function (2.1) provides an image for the boundary of the scatterer, that is, the imaging function has relatively large values on the boundary of the scatterer compared with its values inside or outside the scatterer. Unfortunately, for any given grid point, the imaging function itself does not offer any clear indication whether the grid point is inside or outside the scatterer. To provide an initial guess q for the scatterer, it is crucial to distinguish whether a grid point is inside or outside the scatterer, *i.e.*, the support of q. This can be accomplished by converting the imaging function to a level set representation of the scatterer via image processing.

2.2. Image processing and the level set function

In this section, we describe an image processing to convert the image for the boundary of the scatterer into a level set representation, which leads to an initial guess.

There are many edge detector algorithms in the literature [8,9,17]. Here, we employ a relatively simple approach. Starting with a large domain enclosing the scatterer, we minimize the cost functional

$$C(\partial\Omega) = \int_{\partial\Omega} f(\mathbf{x})\mathrm{d}s, \tag{2.2}$$

where $f(\mathbf{x}) = 1$ if the imaging function $I(\mathbf{x})$ is larger than some threshold and $f(\mathbf{x}) = 100$ otherwise. In other words, on the boundary of the scatterer, f is small. It makes the curve shrink to the boundary of the scatterer by minimizing the functional (2.2). In fact, the function f acts as the weight for the curvature-based force in the curve evolution.

Let $\phi(\mathbf{x})$ be a level set function that characterizes the curve $\partial\Omega$, *i.e.*, $\phi(\mathbf{x}) = 0$ on $\partial\Omega$, $\phi(\mathbf{x}) > 0$ outside Ω; $\phi(\mathbf{x}) < 0$ inside Ω. The cost functional can be formulated as [28]

$$C(\partial\Omega) = W(\phi) = \int_{\mathbb{R}^2} f(\mathbf{x})\delta(\phi)|\nabla\phi|\mathrm{d}\mathbf{x}, \tag{2.3}$$

where δ is the Dirac delta function. Taking the derivative with respect to the evolution time t, we have

$$\frac{\mathrm{d}W}{\mathrm{d}t} = \int_{\mathbb{R}^2}\left(\delta'(\phi)|\nabla\phi|\phi_t + \delta(\phi)\frac{\nabla\phi}{|\nabla\phi|}\cdot\nabla(\phi_t)\right)f(\mathbf{x})\mathrm{d}\mathbf{x}. \tag{2.4}$$

The level set formulation for shape evolution with the normal velocity $v(\mathbf{x})$ is [24]

$$\phi_t = -v(\mathbf{x})|\nabla\phi|. \tag{2.5}$$

By substituting (2.5) into (2.4) and using $\delta'(\phi)\nabla\phi = \nabla(\delta(\phi))$, we obtain

$$\frac{\mathrm{d}W}{\mathrm{d}t} = -\int_{\mathbb{R}^2}\left(v(\mathbf{x})\nabla(\delta(\phi))\cdot\nabla\phi + \delta(\phi)\frac{\nabla\phi}{|\nabla\phi|}\cdot\nabla(v(\mathbf{x})|\nabla\phi|)\right)f(\mathbf{x})\mathrm{d}\mathbf{x}. \tag{2.6}$$

Although the evolution velocity is only defined on the moving curve initially, it can be extended by a constant normal extension away from the curve. Since $\nabla\phi$ is in the normal direction, we have $\nabla v\cdot\nabla\phi = 0$. Therefore, Eq. (2.6) can be rewritten as

$$\frac{\mathrm{d}W}{\mathrm{d}t} = -\int_{\mathbb{R}^2}\left(\nabla(\delta(\phi))\cdot\nabla\phi + \delta(\phi)\frac{\nabla\phi}{|\nabla\phi|}\cdot\nabla(|\nabla\phi|)\right)v(\mathbf{x})f(\mathbf{x})\mathrm{d}\mathbf{x}. \tag{2.7}$$

It follows from the divergence theorem on the first term of the right-hand side of (2.7) that

$$\frac{\mathrm{d}W}{\mathrm{d}t} = \int_{\mathbb{R}^2}\delta(\phi)\left(\nabla\cdot(v(\mathbf{x})f(\mathbf{x})\nabla\phi) - \frac{\nabla\phi}{|\nabla\phi|}\cdot\nabla(|\nabla\phi|)v(\mathbf{x})f(\mathbf{x})\right)\mathrm{d}\mathbf{x}. \tag{2.8}$$

Simple calculations from the product rule yield

$$\frac{\mathrm{d}W}{\mathrm{d}t} = \int_{\mathbb{R}^2}\delta(\phi)|\nabla\phi|v(\mathbf{x})\nabla\cdot\left(f(\mathbf{x})\frac{\nabla\phi}{|\nabla\phi|}\right)\mathrm{d}\mathbf{x}, \tag{2.9}$$

which can be written as a curve integral

$$\frac{\mathrm{d}W}{\mathrm{d}t} = \int_{\partial\Omega}v(\mathbf{x})\nabla\cdot\left(f(\mathbf{x})\frac{\nabla\phi}{|\nabla\phi|}\right)\mathrm{d}s. \tag{2.10}$$

Let $v(\mathbf{x}) = -\nabla\cdot\left(f(\mathbf{x})\frac{\nabla\phi}{|\nabla\phi|}\right)$. By substituting it into (2.5), we arrive at the gradient flow for the level set function

$$\phi_t = |\nabla\phi|\nabla\cdot\left(f(\mathbf{x})\frac{\nabla\phi}{|\nabla\phi|}\right). \tag{2.11}$$

By using such a normal velocity, we always have $\mathrm{d}W/\mathrm{d}t < 0$, *i.e.*, the cost functional decreases monotonically in the shape evolution. In practice, a local level set method [25] with reinitialization using a time marching scheme [26] is employed for solving (2.11).

Starting with a box containing all scatterers, the evolution will stop at the convex envelope of the shapes for scatterers in the MUSIC imaging result. The level set function representing the shape of the envelope may be selected as an initial guess.

3. Recursive linearization

Once an initial guess is obtained as described in the previous section, we perform recursive linearization to improve the reconstruction for the scatterers: suppose now that the scatterer $q_{\tilde{k}}$ has been recovered at some wavenumber $\tilde{k}$, and that the wavenumber k is slightly larger that $\tilde{k}$. We wish to determine q_k, or equivalently, to determine the perturbation

$$\delta q = q_k - q_{\tilde{k}}.$$

For the reconstructed scatterer $q_{\tilde{k}}$, we solve at the wavenumber k the forward scattering problem

$$\Delta\tilde{u}_i^{\mathrm{s}} + k^2(1+q_{\tilde{k}})\tilde{u}_i^{\mathrm{s}} = -k^2 q_{\tilde{k}}u_i^{\mathrm{i}}, \tag{3.1}$$

where u_i^{i} is the incident wave with the incident angle $\mathbf{d}_i$, $i = 1,\ldots,m$. For the scatterer q_k, we have

$$\Delta u_i^{\mathrm{s}} + k^2(1+q_k)u_i^{\mathrm{s}} = -k^2 q_k u_i^{\mathrm{i}}. \tag{3.2}$$

Subtracting (3.1) from (3.2) and omitting the second order smallness in δq and in $\delta u_i^{\mathrm{s}} = u_i^{\mathrm{s}} - \tilde{u}_i^{\mathrm{s}}$, we obtain

$$\Delta\delta u_i^{\mathrm{s}} + k^2(1+q_{\tilde{k}})\delta u_i^{\mathrm{s}} = -k^2\delta q(u_i^{\mathrm{i}} + \tilde{u}_i^{\mathrm{s}}). \tag{3.3}$$

Given a solution u_i^{s} of (3.2), we define the measurements

$$Mu_i^{\mathrm{s}}(\mathbf{x}) = [u_i^{\mathrm{s}}(\mathbf{x}_1), \ldots, u_i{}^{\mathrm{s}}(\mathbf{x}_m)]^{\mathrm{T}}. \tag{3.4}$$

The measurement operator M maps the scattered fields to a vector of complex numbers in $\mathbb{C}^m$, which consists of point measurements of the scattered field at $\mathbf{x}_j$, $j = 1,\ldots,m$.

For the scatterer q_k and the incident field u_i^{i}, we define the forward scattering operator

$$S(q_k, u_i^{\mathrm{i}}) = Mu_i^{\mathrm{s}}. \tag{3.5}$$

It is easily seen that the forward scattering operator $S(q_k, u_i{}^{\mathrm{i}})$ is linear with respect to u_i^{i} but nonlinear with respect to q_k. For simplicity, we denote $S(q_k, u_i^{\mathrm{i}})$ by $S_i(q_k)$. Let $S_i'(q_{\tilde{k}})$ be the Fréchet derivative of $S_i(q_k)$ and denote the residual operator

$$R_i(q_{\tilde{k}}) = M(\delta u_i^{\mathrm{s}}). \tag{3.6}$$

It follows from the linearization of the nonlinear equation (3.5) that

$$S_i'(q_{\tilde{k}})\delta q = R_i(q_{\tilde{k}}). \tag{3.7}$$

Applying the Landweber iteration [14] to the linearized equation (3.7) yields

$$\delta q = \beta S_i'(q_{\tilde{k}})^* R_i(q_{\tilde{k}}), \tag{3.8}$$

where β is a positive relaxation parameter and $S_i'(q_{\tilde{k}})^*$ is the adjoint operator of $S_i'(q_{\tilde{k}})$.

Let $R_i(q_{\tilde{k}}) = [\zeta_{i1}, \ldots, \zeta_{im}]^{\mathrm{T}} \in \mathbb{C}^m$. Consider the adjoint problem

$$\Delta\psi_i + k^2(1 + q_{\tilde{k}})\psi_i = -k^2 \sum_{j=1}^{m} \zeta_{ij}\delta(\mathbf{x} - \mathbf{x}_j). \tag{3.9}$$

In order to compute the correction δq, we need an efficient way to compute $S_i'(q_{\tilde{k}})^* R_i(q_{\tilde{k}})$, which is given by the following theorem. See [6] for a complete proof.

Theorem 3.1. *Given residual $R_i(q_{\tilde{k}})$, there exists a solution ψ_i of (3.9) such that*

$$[S_i'(q_{\tilde{k}})^* R_i(q_{\tilde{k}})](\mathbf{x}) = (\overline{u_i^{\mathrm{i}}}(\mathbf{x}) + \overline{\tilde{u}_i^{\mathrm{s}}}(\mathbf{x}))\psi_i(\mathbf{x}), \tag{3.10}$$

where the overline denotes the complex conjugate, u_i^{i} is the incident wave, and $\tilde{u}_i^{\mathrm{s}}$ is the solution of (3.1).

Using the above result, Eq. (3.8) can be written as

$$\delta q = \beta(\overline{u_i^{\mathrm{i}}} + \overline{\tilde{u}_i^{\mathrm{s}}})\psi_i. \tag{3.11}$$

Thus, for each incident wave, we solve one forward problem (3.1) and one adjoint problem (3.9). Once δq is determined, q_k is updated by $q_{\tilde{k}} + \delta q$. After completing the mth sweep, *i.e.*, all incident directions, we get the reconstructed scatterer q_k at the wavenumber k.

4. Numerical experiments

Three numerical examples are presented to illustrate the performance of the proposed method. Here, the scattering data is generated by numerical solution of the forward scattering problem, which is implemented by using the finite element method with a perfectly matched layer technique [27].

The scattered fields are measured on the boundary $\mathbf{x} \in \partial D$, where $D = [-5, 5] \times [-5, 5]$, and the incident angle $\theta_i = i2\pi/20$, $i = 1,\ldots,20$. The constant q_0 inside and the relaxation parameter β are taken to be 1 and $0.01/k^2$, respectively. To test the stability, some relative random noise is added to the data, *i.e.*, the scattered field takes the form

$$u^{\mathrm{s}}|_{\partial D} := (1 + \sigma \text{ rand})u^{\mathrm{s}}|_{\partial D},$$

where rand gives uniformly distributed random numbers in $[-1, 1]$ and σ is a noise level parameter taken to be 0.05 in our numerical experiments.

The initial guesses are obtained via the MUSIC algorithm and a level set representation at the wavenumber $k = 1$. This is chosen to be a low frequency such that the MUSIC algorithm gives a robust estimate. The largest wavenumber used in the recursive linearization algorithm is $k = 6$. The step size for wavenumbers is 0.5, *i.e.*, the number of iteration along wavenumbers is 10. The computational cost is affordable.

Example 1. Reconstruction of a five-leave shape scatterer as shown in Fig. 1a. Fig. 1b exhibits the initial guess as a level set function obtained via image processing for the MUSIC imaging function while Fig. 1c shows the final reconstruction.

Example 2. Reconstruction of a five-leave shape scatterer with a disc of radius 1 removed, Fig. 2a. Fig. 2b shows the initial guess as a level set function while Fig. 2c presents the final reconstruction.

Example 3. Reconstruction of three isolated kite shape scatterers as shown in Fig. 3a. Fig. 3b shows the initial guess as a level set function while Fig. 3c exhibits the final reconstruction.

From these examples, it is evident that the MUSIC algorithm, though a fast direct algorithm, does not provide detailed shape information from the initial frequency data. In particular, it cannot capture the holes for multiply connected scatterers. However, it does provide reasonable initial guesses that lead to excellent final reconstructions through recursive linearization.

One might be tempted to use higher frequency for the initial guesses so that the MUSIC imaging function gives more details. However, the higher frequency we use as the initial frequency, the less robust the reconstruction is.

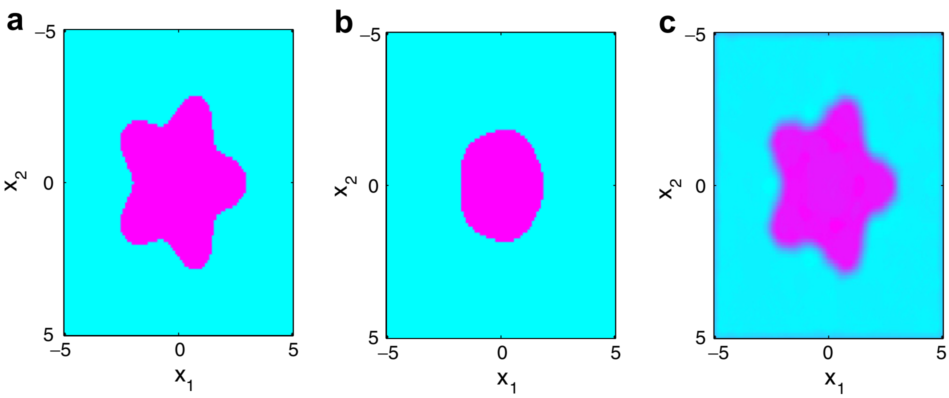

Fig. 1. Example 1: (a) the true scatterer; (b) the initial guess; and (c) the final reconstruction.

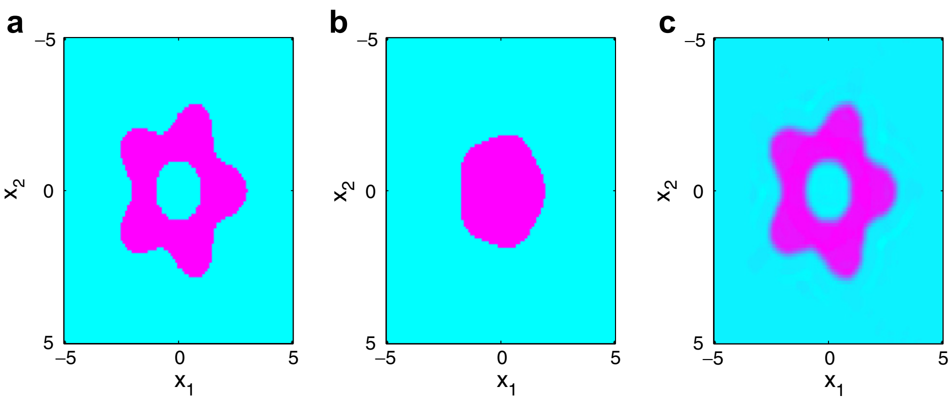

Fig. 2. Example 2: (a) the true scatterer; (b) the initial guess; and (c) the final reconstruction.

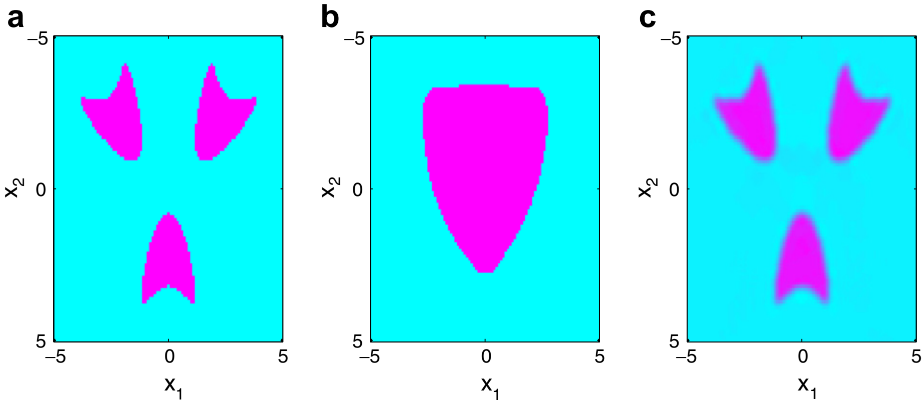

Fig. 3. Example 3: (a) the true scatterer; (b) the initial guess; and (c) the final reconstruction.

5. Concluding remarks

We have presented a continuation method with respect to the wavenumbers. Starting from an initial guess via the MUSIC algorithm and a level set representation, each update is obtained by solving essentially two forward scattering problems. The proposed method is accurate, efficient, and robust: compared with the direct imaging methods such as the MUSIC algorithm and the linear sampling method, the proposed method is capable of imaging multiply connected medium; Compared with the iterative imaging methods, the proposed method starts with an initial guess with a frequency where Born approximation may not be valid, therefore lower frequency iterations would not be needed in the computation; Numerical experiments show the robustness of the method with respect to noisy data.

Furthermore, the method has the potential to solve the general inverse medium problem. For simplicity, we assumed that the inhomogeneity q takes a given constant value in its support. In fact, as long as a reasonable guess for the function q is given, the method is capable of reconstructing q that is not a constant. Unfortunately the MUSIC imaging algorithm is unable to provide a guess for the function value of q: it barely provides a guess for the support of q.

A related ongoing project is to investigate the inverse obstacle scattering problem, which reconstructs the interface of the scatterer (obstacle) in both two and three dimensions.

Acknowledgments

We thank Professors Hongkai Zhao and Knut Solna for useful discussions.

References

[1] H. Ammari, H. Kang, Reconstruction of Small Inhomogeneities from Boundary Measurements, Lecture Notes in Mathematics, vol. 1846, Springer, NY, 2004.
[2] G. Bao, J. Liu, Numerical solution of inverse problems with multi-experimental limited aperture data, SIAM J. Sci. Comput. 25 (2003) 1102–1117.
[3] G. Bao, P. Li, Inverse medium scattering for three-dimensional time harmonic Maxwell equations, Inverse Probl. 20 (2004) L1–L7.
[4] G. Bao, P. Li, Inverse medium scattering problems for electromagnetic waves, SIAM J. Appl. Math. 65 (2005) 1066–2049.
[5] G. Bao, P. Li, Inverse medium scattering for the Helmholtz equation at fixed frequency, Inverse Probl. 21 (2005) 1621–1641.
[6] G. Bao, P. Li, Inverse medium scattering problems in near-field optics, J. Comput. Math. 25 (3) (2007) 252–265.
[7] G. Bao, P. Li, Numerical solution of inverse scattering for near-field optics, Opt. Lett. 32 (11) (2007) 1465–1467.
[8] V. Caselles, F. Catte, T. Coll, F. Dibos, A geometric model for active contours in image processing, Numer. Math. 66 (1993) 1–31.
[9] V. Casseles, R. Kimmel, G. Sapiro, On geodesic active contours, Int. J. Comput. Vis. 22 (1997) 61–79.
[10] Y. Chen, Inverse scattering via Heisenberg uncertainty principle, Inverse Probl. 13 (1997) 253–282.
[11] Y. Chen, Inverse scattering via skin effect, Inverse Probl. 13 (1997) 649–667.
[12] D. Colton, R. Kress, Inverse Acoustic and Electromagnetic Scattering Theory, Appl. Math. Sci., second ed., vol. 93, Springer-Verlag, Berlin, 1998.

[13] O. Dorn, E. Miller, C. Rappaport, A shape reconstruction method for electromagnetic tomography using adjoint fields and level sets, Inverse Probl. 16 (2000) 1119–1156.
[14] H. Engl, M. Hanke, A. Neubauer, Regularization of Inverse Problems, Kluwer, Dordrecht, 1996.
[15] F.K. Gruber, E.A. Marengo, A.J. Devaney, Time-reversal imaging with multiple signal classification considering multiple scattering between the targets, J. Acoust. Soc. Am. 115 (2004) 3042–3047.
[16] K. Ito, K. Kunisch, Z. Li, Level-set function approach to an inverse interface problem, Inverse Probl. 17 (2001) 1225–1242.
[17] M. Kass, A. Witkin, D. Terzopoulos, Snakes: active contour models, Int. J. Comput. Vis. 1 (1988) 321–331.
[18] R. Kress, W. Rundell, Inverse scattering for shape and impedance, Inverse Probl. 17 (2001) 1075–1085.
[19] F. Hassen, J. Liu, R. Potthast, On source analysis by wave splitting with applications in inverse scattering of multiple obstacles, J. Comput. Math. 25 (3) (2007) 266–281.
[20] S. Hou, K. Solna, H. Zhao, A direct imaging algorithm for extended targets, Inverse Probl. 22 (2006) 1151–1178.
[21] A. Litman, D. Lesselier, F. Santosa, Reconstruction of a two-dimensional binary obstacle by controlled evolution of a level set, Inverse Probl. 14 (1998) 685–706.
[22] P.S. Meyer, M. Capistran, Y. Chen, On the naturally induced sources for obstacle scattering, Commun. Comput. Phys. 1 (6) (2006) 974–983.
[23] F. Natterer, F. Wübbeling, A propagation–backpropagation method for ultrasound tomography, Inverse Probl. 11 (1995) 1225–1232.
[24] S. Osher, J. Sethian, Fronts propagating with curvature-dependent speed: algorithms based on Hamilton–Jacobi formulations, J. Comput. Phys. 79 (1988) 12–49.
[25] D. Peng, B. Merriman, S. Osher, H. Zhao, M. Kang, A PDE-based fast local level set method, J. Comput. Phys. 155 (2) (1999) 410–438.
[26] M. Sussman, P. Smereka, S. Osher, A level set approach for computing solutions to incompressible two-phase flows, J. Comput. Phys. 119 (1994) 146–159.
[27] S.V. Tsynkov, E. Turkel, A Cartesian perfectly matched layer for the Helmholtz equation, in: L. Tourrette, L. Halpern (Eds.), Absorbing Boundaries and Layers, Domain Decomposition Methods, Applications to Large Scale Computations, Nova Science Publishers, New York, 2001, pp. 279–309.
[28] H. Zhao, T. Chan, B. Merriman, S. Osher, A variational level set approach to multiphase motion, J. Comput. Phys. 127 (1996) 179–195.